THE COMPANY OF
Biologists

RESEARCH ARTICLE

Sharp-1 regulates TGF-β signaling and skeletal muscle regeneration

Sujata Acharjee[1],*, Teng-Kai Chung[1,2], Suma Gopinadhan[2], Shilpa Rani Shankar[2], Yaju Wang[2], Li Li[1], Cecile Vercherat[1], Neriman Tuba Gulbagci[1], Moritz Rossner[3] and Reshma Taneja[1,2,*]

ABSTRACT

Sharp-1 is a basic helix-loop-helix (bHLH) transcriptional repressor that is involved in a number of cellular processes. Our previous studies have demonstrated that Sharp-1 is a negative regulator of skeletal myogenesis and it blocks differentiation of muscle precursor cells by modulating the activity of MyoD. In order to understand its role in pre- and post-natal myogenesis, we assessed skeletal muscle development and freeze-injury-induced regeneration in Sharp-1-deficient mice. We show that embryonic skeletal muscle development is not impaired in the absence of Sharp-1; however, post-natally, the regenerative capacity is compromised. Although the initial phases of injury-induced regeneration proceed normally in Sharp-1$^{-/-}$ mice, during late stages, the mutant muscle exhibits necrotic fibers, calcium deposits and fibrosis. TGF-β expression, as well as levels of phosphorylated Smad2 and Smad3, are sustained in the mutant tissue and treatment with decorin, which blocks TGF-β signaling, improves the histopathology of Sharp-1$^{-/-}$ injured muscles. *In vitro*, Sharp-1 associates with Smad3, and its overexpression inhibits TGF-β- and Smad3-mediated expression of extracellular matrix genes in myofibroblasts. These results demonstrate that Sharp-1 regulates muscle regenerative capacity, at least in part, by modulation of TGF-β signaling.

KEY WORDS: TGF-β, Fibrosis, Regeneration, Skeletal muscle, Degeneration, Myofibroblast

INTRODUCTION

Regeneration is a feature of postnatal skeletal muscle and occurs to replace damaged myofibers following exercise or injury (Hawke and Garry, 2001; Huard et al., 2002; Chargé and Rudnicki, 2004). Regeneration of muscle is dependent on satellite cells, and can be divided into distinct phases, which include inflammation, tissue formation and tissue remodeling. During the inflammatory phase, the damaged muscle tissue is infiltrated by immune cells, and activated macrophages play a key role in the removal of necrotic tissue. This is followed by tissue formation that is dependent on the proliferation and differentiation of satellite cells. Many growth factors and cytokines that are mitogenic for satellite cells have been implicated in this process (Husmann et al., 1996). The progeny of activated satellite cells

are called muscle precursor cells and they undergo multiple rounds of proliferation, withdraw from the cell cycle and differentiate to form myotubes that are characterized by the presence of a centrally located nuclei (Huard et al., 2002; Chargé and Rudnicki, 2004). Further growth and fusion results in the formation of myofibers. During tissue remodeling, fibroblasts present at the site of injury produce an initial extracellular matrix (ECM) of type I and type III collagens. Differentiation of fibroblasts into myofibroblasts augments their contractile activity (Border and Ruoslahti, 1992; Border and Noble, 1994; Grinnell, 1994). Myofibroblasts also produce ECM, further contributing to tissue remodeling. Once the tissue is repaired, the contractile activity of myofibroblasts is terminated and cells are removed by apoptosis. Myofibroblast persistence and excessive fibroblast proliferation can result in the formation of scar tissue (fibrosis), which is a sign of incomplete regeneration, and is often accompanied by elevated TGF-β levels and collagen deposition (Desmoulière et al., 1993; Serini and Gabbiani, 1996; Serini et al., 1998). In myopathies such as Duchenne muscular dystrophy (DMD), the regeneration process is compromised, and muscle tissue is replaced by dysfunctional scar (fibrotic) tissue. Levels of TGF-β1 and TGF-β2 are elevated in muscular dystrophies and have been shown to cause fibrosis in dystrophic muscles (Bernasconi et al., 1995; Bernasconi et al., 1999; Murakami et al., 1999; Zhu et al., 2007). Interestingly, inhibition of TGF-β signaling not only prevents fibrosis, but also improves regeneration in mdx mutants that are widely studied as a mouse model for DMD (Lefaucheur and Sébille, 1995; Cohn et al., 2007), indicating that regulation of fibrosis presents a key step in the pathology of DMD.

Members of the TGF-β superfamily are multifunctional cytokines that regulate diverse physiological processes including development, homeostasis, wound healing, differentiation, apoptosis and cell cycle arrest (Barnard et al., 1990; Moses et al., 1990). In general, TGF-β inhibits proliferation of most cells and induces apoptosis of epithelial cells. By contrast, TGF-β stimulates fibroblast cells to proliferate and produce ECM that results in a fibrotic response in tissues. TGF-β signals through heteromeric transmembrane type I and type II receptors (Wrana et al., 1992; Heldin et al., 1997). In the presence of TGF-β ligand, the receptor-activated Smad proteins Smad2 and Smad3, are phosphorylated (pSmad2/3), bind to the common Smad (Smad4) and translocate into the nucleus (Wrana et al., 1992; Massaous et al., 1997). Nuclear Smad protein complexes bind specific DNA sequence motifs and recruit coactivators such as CBP/p300 and participate in transcriptional regulation of target genes (Massaous et al., 1997), including those encoding ECM proteins. Excessive TGF-β-induced deposition of ECM at the site of injury can lead to fibrosis (Serini and Gabbiani, 1996; Serini et al., 1998). Although

[1]Department of Developmental and Regenerative Biology, Mount Sinai School of Medicine, One Gustave L. Levy Place, New York, NY 10029, USA. [2]Department of Physiology, National University of Singapore, 117597 Singapore. [3]Molecular and Behavioral Neurobiology, Department of Psychiatry Nussbaumstr, 780336 München, Germany.

*Authors for correspondence (sujataacharjee@yahoo.com; phsrt@nus.edu.sg)

several pathways are implicated in regulation of the distinct steps in muscle regeneration, the molecular mechanisms governing regeneration and repair are not fully understood.

Sharp-1 (also known as Dec2 and BHLHE41) is a basic helix-loop-helix transcription factor that plays complex roles in cellular differentiation, apoptosis, cell cycle arrest, tumor progression and circadian rhythms (Yamada and Miyamoto, 2005; Sun et al., 2007a). Our previous studies have shown that overexpression of Sharp-1 in myoblasts or preadipocytes blocks their ability to undergo terminal differentiation (Azmi et al., 2004; Gulbagci et al., 2009; Ling et al., 2012; Wang et al., 2013). Here, we demonstrate that Sharp-1 plays a role in skeletal muscle regeneration by regulating TGF-β signaling. In response to injury, Sharp-1 null mutants exhibit a defect at late stages of regeneration. Sustained TGF-β expression increases levels of pSmad2/3 and myofibroblasts positive for smooth muscle actin (SMA$^+$) in Sharp-1$^{-/-}$ regenerating tissue. Inhibition of TGF-β signaling ameliorates muscle pathology and degeneration in Sharp-1$^{-/-}$ mice. We demonstrate that Sharp-1 directly regulates TGF-β signaling and antagonizes Smad3-dependent expression of collagens and tissue inhibitor of metalloproteinase 1 (TIMP1) probably by interacting with Smad3 and inhibiting its transcriptional activity. Taken together, our studies indicate that Sharp-1 is essential to limit TGF-β and Smad3 signaling in myofibroblast cells and this impacts skeletal muscle regeneration.

RESULTS

Skeletal muscle development in Sharp-1$^{-/-}$ mice

We have previously demonstrated that Sharp-1 is expressed in skeletal muscles during embryonic development, as well as in adult tissues, and its overexpression inhibits myogenesis through regulation of MyoD activity (Azmi et al., 2003; Azmi et al., 2004; Ling et al., 2012; Wang et al., 2013). To further examine the role of endogenous Sharp-1, we analyzed embryonic and postnatal myogenesis in wild-type (WT) and littermate Sharp-1-null (Sharp-1$^{-/-}$) mutant mice (Rossner et al., 2008). No overt difference in myogenin expression was apparent in WT and Sharp-1$^{-/-}$ embryos at embryonic (E) day 16.5 (Fig. 1A). Histological analysis of quadriceps muscles from adult WT and Sharp-1$^{-/-}$ mice also did not reveal any obvious defects in muscle architecture (Fig. 1B) or in the mean cross-section area (CSA) (Fig. 1C, right panel), indicating that the development of skeletal muscles occurs normally in the absence of Sharp-1. Moreover, no changes in the number of Pax7$^+$ satellite cells was noted between WT and Sharp-1$^{-/-}$ mutants (Fig. 1D,E).

Skeletal muscle regeneration is impaired in Sharp-1-null mutants

We then examined the regenerative potential of Sharp-1-null mutants in response to freeze injury. Quadriceps muscles from 2- to 3-month-old WT and Sharp-1$^{-/-}$ mice were injured (Sun et al., 2007b) and regeneration was analyzed histologically. Hematoxylin and eosin (HE) staining of injured muscle sections revealed extensive myofiber damage in both WT and Sharp-1$^{-/-}$ mice at D2, with no marked histological differences apparent at this stage (data not shown). Five days after injury (D5), regeneration was evident in both WT and Sharp-1$^{-/-}$ muscles with the presence of newly formed myotubes containing central nuclei (Fig. 2A). Ten and sixteen days (D10 and D16 respectively) post injury, regeneration in WT mice was evident by presence of centrally nucleated newly formed myotubes. In
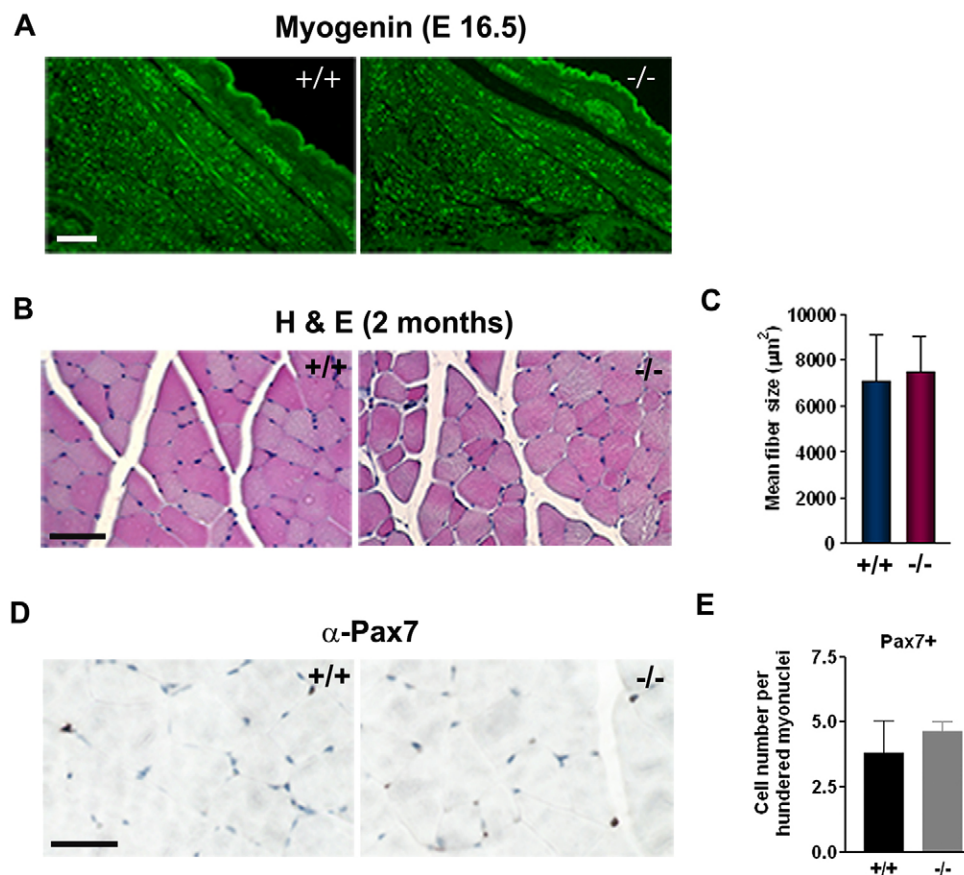

Fig. 1. Development of skeletal muscle in Sharp-1$^{-/-}$ mutants. (A) Embryonic myogenesis in WT (+/+) and Sharp-1$^{-/-}$ ($^{-/-}$) embryos at E16.5 was analyzed by immunostaining with anti-myogenin antibody followed by fluorescence microscopy. (B) Quadriceps muscles from 2-month-old WT (+/+) and Sharp-1$^{-/-}$ ($^{-/-}$) mice (n=4) were analyzed histologically by H&E staining. (C) H&E-stained sections of quadriceps muscles were used to determine the cross-section area of myofibers in both genotypes (n=4). The mean fiber size was not significantly different between WT and Sharp-1$^{-/-}$ mice. Data are mean ± s.e. (D) WT and Sharp-1$^{-/-}$ muscles were immunostained with anti-Pax7 antibody to detect satellite cells. Sections were counterstained with hematoxylin. (E) Pax7-stained muscle sections were used to analyze the percentage of satellite cells from four independent WT and Sharp-1$^{-/-}$ mice. Scale bars: 100 μm.

contrast to WT muscles, the mutant tissue revealed overt signs of necrosis and degeneration (Fig. 2A). Indeed, mutant quadriceps muscles stained positively with Alizarin Red, indicating calcification, which is a hallmark of dystrophic tissues (Fig. 2B). In addition, fibrosis was detectable in the mutant regenerating muscles by Masson's Trichrome staining (Fig. 2C).

To examine the mechanisms underlying defective regeneration in Sharp-1$^{-/-}$ muscle, we first analyzed the expression of MyoD, which is a marker of proliferating myoblasts. MyoD levels were upregulated during regeneration in both WT and Sharp-1$^{-/-}$ mutants as seen by western blot analysis (Fig. 3A). Immunostaining of D10 injured tissue revealed many MyoD^{+} cells in the mutant tissue compared with WT muscle. Moreover, several smooth-muscle-actin-positive (SMA^{+}), cells were also

apparent in Sharp-1$^{-/-}$ muscle that did not colocalize with MyoD^{+} cells, indicating the presence of myofibroblasts in the mutant tissue (Fig. 3B). We then examined differentiation using an embryonic MHC (eMHC) antibody. Immunostaining of injured WT and Sharp-1$^{-/-}$ muscle at D5 revealed a higher number of eMHC^{+} myotubes in the mutant tissue, which correlated with a higher regeneration index (Fig. 3C,D). Together, these results suggest that the compromised regeneration at late stages (D10/D16) is not due to a differentiation defect, but might reflect an additional role for Sharp-1 in the late steps of tissue remodeling.

Increased TGF-β signaling in Sharp-1$^{-/-}$ injured muscles

Upon activation by ligand, TGF-β receptors induce phosphorylation of Smad2 and Smad3, which form a
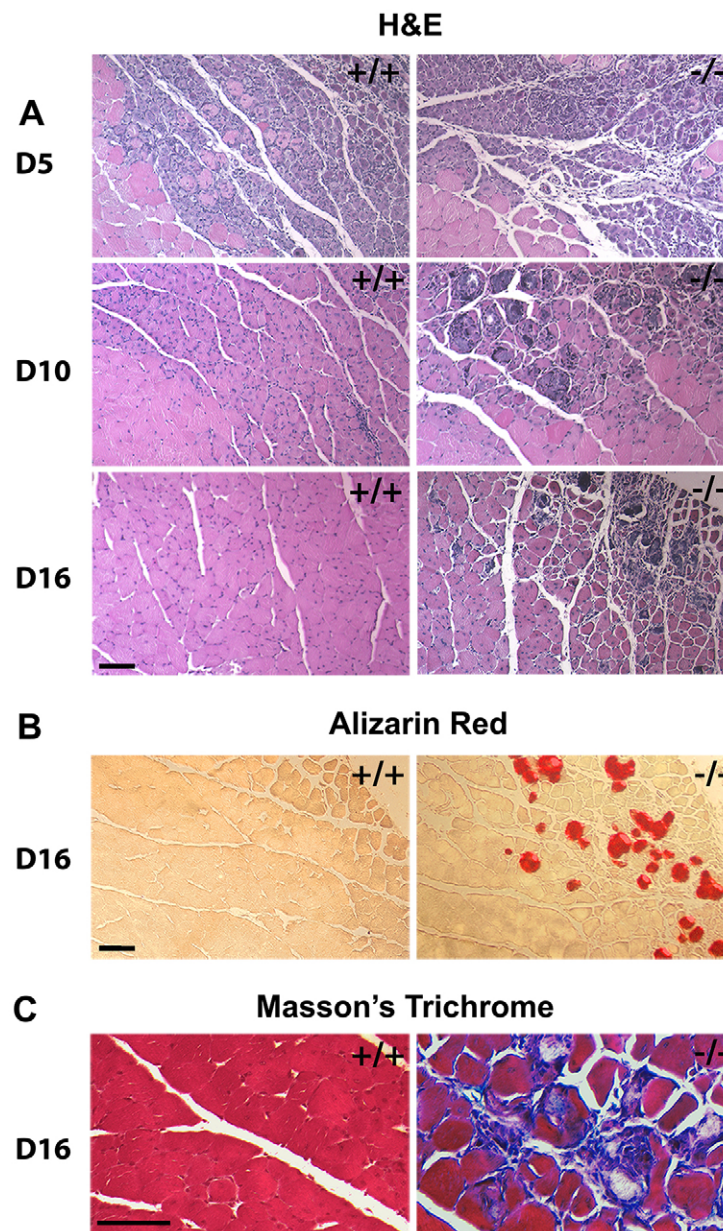

Fig. 2. Altered regenerative response upon freeze injury in Sharp-1$^{-/-}$ mice. (A) Histological analysis of muscle regeneration in WT (+/+) and Sharp-1$^{-/-}$ ($^{-/-}$) mice at D5, D10 and D16 following injury. At D5, newly formed myotubes with central nuclei are evident in both WT and mutant muscles. At later stages (D10 and D16 after injury), muscle degeneration is apparent in Sharp-1$^{-/-}$ mutants. (B,C) Alizarin Red staining (B), and Masson's Trichrome staining (C), at D16 after injury revealed the presence of calcium deposits and collagen deposition (blue staining) respectively in Sharp-1$^{-/-}$ muscles. Scale bars: 100 µm.
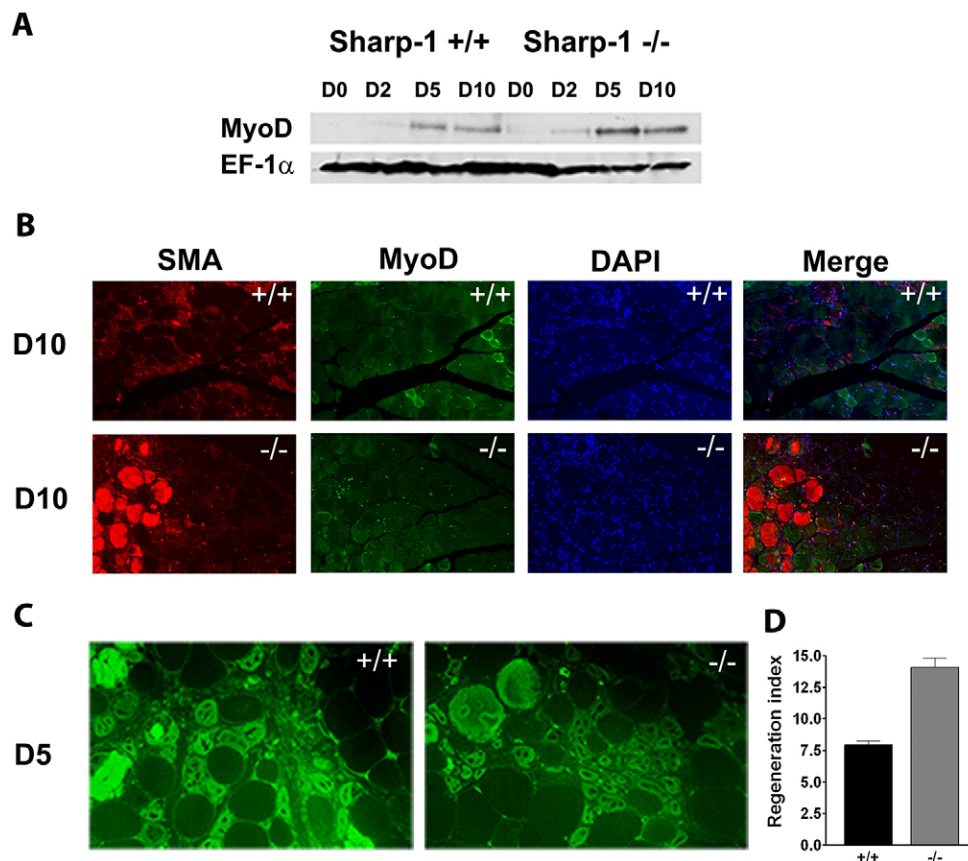
Fig. 3. Myogenic differentiation is not altered in Sharp-1$^{-/-}$ muscles.
(A) Western blotting was performed with protein lysates from WT (+/+) and Sharp-1$^{-/-}$ ($^{-/-}$) uninjured (D0) and injured tissues (D2, D5 and D10 after injury) to detect MyoD expression. EF1α was used as an internal control. (B) Sections of quadriceps muscles from WT and Sharp-1$^{-/-}$ mice at D10 after injury were immunostained with anti-MyoD and anti-SMA antibodies. (C) Sections of quadriceps muscles from WT and Sharp-1$^{-/-}$ mice at D5 after injury were stained with anti-eMHC antibody. (D) Regeneration index was calculated by determining the percentage of eMHC$^+$ myotubes in WT and Sharp-1$^{-/-}$ mice ($n=4$). Data are means ± s.e.

heterotrimeric complex with Smad4 and then translocate to the nucleus (Wrana et al., 1992). Estimation of pSmad2/3 levels thus serves as a measure of TGF-β signaling. Because Sharp-1$^{-/-}$ mutants exhibit fibrosis, we examined TGF-β expression levels by western blot analysis in WT and Sharp-1$^{-/-}$ muscles at various time points after injury (Fig. 4A). In WT mice, TGF-β expression was strongly induced upon injury, with elevated levels apparent at D2, and the levels started to decline at D5 and D10. By contrast, TGF-β expression was sustained at high levels at D5 and D10 in Sharp-1-null mutants. To examine whether the increased TGF-β resulted in increased signaling, we analyzed pSmad2/3 levels by immunostaining (Fig. 4B). Interestingly, in correlation with increased TGF-β levels, pSmad2/3 levels were also higher in Sharp-1$^{-/-}$ injured muscles at D5 and D10 compared with WT muscles (Fig. 4B). TGF-β induces differentiation of myofibroblasts that play a crucial role in fibrosis (Desmoulière et al., 1993; Li et al., 2004). Consistent with sustained high levels of TGF-β signaling, the mutant tissue exhibited an increased number of SMA$^+$ cells at D5 and D10 after injury (Fig. 4C) which was in contrast to WT tissue, where few SMA$^+$ myofibroblasts were apparent at any stage.

Inhibition of TGF-β signaling ameliorates muscle necrosis
Previous studies have demonstrated that blocking TGF-β can improve muscle pathology in mdx mice (Cohn et al., 2007) and one such blocker that has been successfully used against fibrosis in mice is the proteoglycan decorin (Isaka et al., 1996; Li et al., 2007). To assess whether the enhanced TGF-β signaling underlies muscle necrosis in Sharp-1$^{-/-}$ mice, we injected decorin in Sharp-1$^{-/-}$ muscle and performed histological analysis 3 days later. The contralateral muscle was injected with PBS. Decorin-injected

injured muscles from Sharp-1$^{-/-}$ mice showed a considerable decrease in degenerating myofibers and a significant increase in regenerating myofibers (Fig. 5A). Quantification of the damaged area indicated reduced pathology in decorin-injected muscles relative to uninjected muscle (Fig. 5B). To confirm that decorin indeed led to reduced TGF-β signaling, uninjected and injected injured muscles were immunostained with pSmad2/3 antibody (Fig. 5C). As expected, pSmad2/3 staining was higher in uninjected tissue compared with that injected with decorin. Moreover, consistent with inhibition of TGF-β activity, SMA$^+$ cells were also reduced in decorin-treated muscle (Fig. 5D).

Sharp-1 regulates TGF-β signaling
To examine the mechanisms that might account for deregulated TGF-β expression and signaling, we first investigated whether Sharp-1 interacts with components of the pathway. The interaction of Sharp-1 with Smad3, a key mediator of the TGF-β response was analyzed. Myc-tagged Sharp-1 was transfected in cells, and lysates were harvested in the absence and presence of TGF-β. An interaction of Sharp-1 with endogenous pSmad2/3 and total Smad2/3 was apparent in the presence of TGF-β (Fig. 6A). To define the domains in Sharp-1 that associate with Smad3, various Sharp-1 deletion mutants (Ling et al., 2012) were transfected, alone or with Smad3. Immunoprecipitation assays indicated that full-length Sharp-1, and the deletion mutants Sharp-1ΔC, lacking the C-terminal region, and Sharp-1ΔO, which lacks the orange domain, interacted with Smad3. However, no association was seen with the Sharp-1-bHLH mutant, which lacks the bHLH domain, indicating that the region essential for interaction with Smad3 resides between amino acids 173–265 of Sharp-1 (Fig. 6B). Moreover, Sharp-1 colocalized
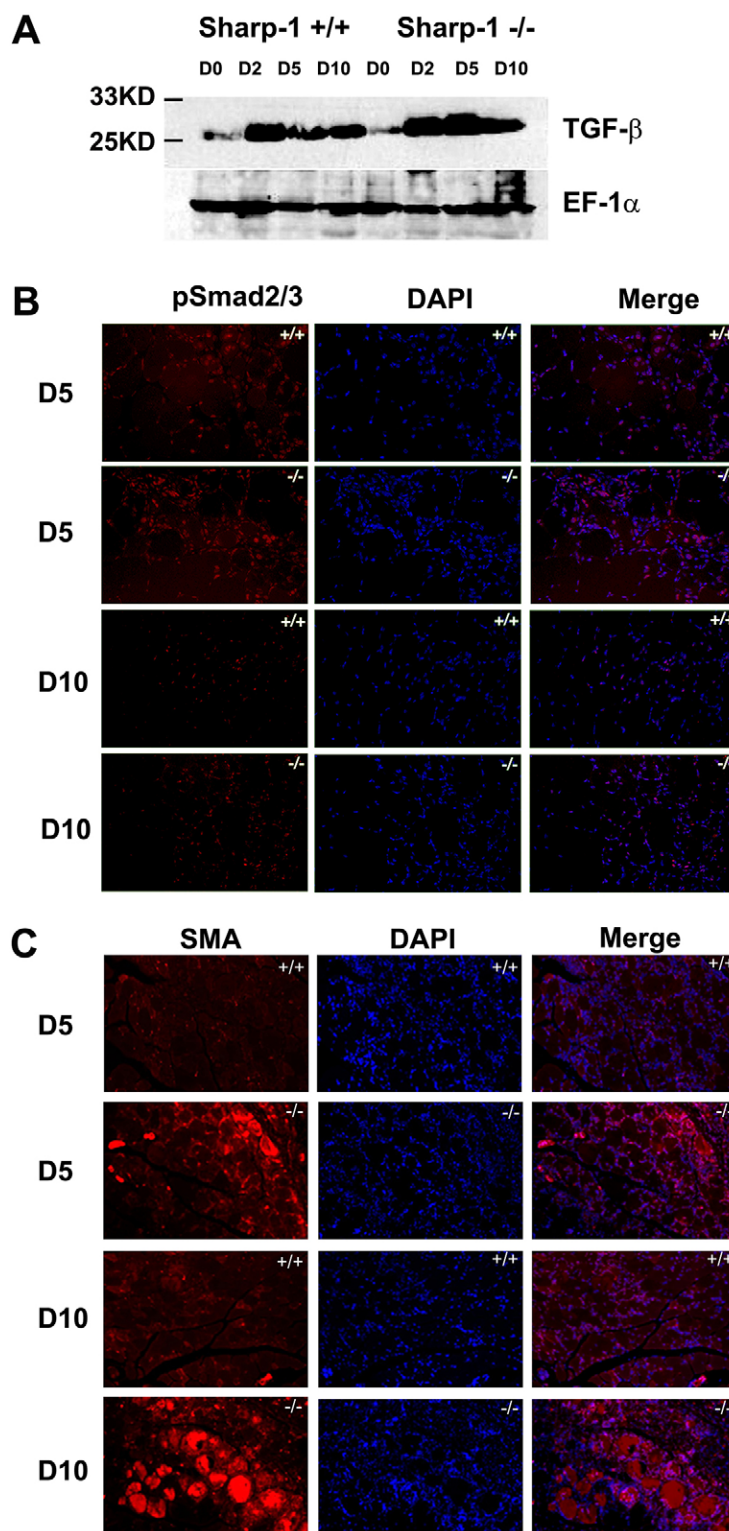
Fig. 4. Increased TGF-β and pSmad2/3 levels in Sharp-1$^{-/-}$ regenerating tissue. (A) Western blotting was performed with protein extracts from WT and Sharp-1$^{-/-}$ regenerating muscle (n=4) after 2, 5 and 10 days of injury and analyzed using anti-TGF-β antibody. EF1α was used as an internal control. (B,C) Sections of injured muscles from WT and Sharp-1$^{-/-}$ mice were immunostained with antibodies against pSmad2/3 (B) and SMA (C) at D5 and D10 after injury.

with Smad3 in the presence of TGF-β (Fig. 6C). To determine whether Sharp-1 directly interacts with Smad3, we performed GST pull-down assays. Equivalent amounts of GST–Sharp-1 or GST protein alone were incubated with ^{35}S-labeled Smad3.

Sharp-1 directly interacted with Smad3, whereas, as expected, no interaction of Smad3 was apparent with GST protein (Fig. 6D).

We next investigated the effect of Sharp-1 expression on TGF-β and Smad3-dependent transcriptional responses using the 3TP-Lux
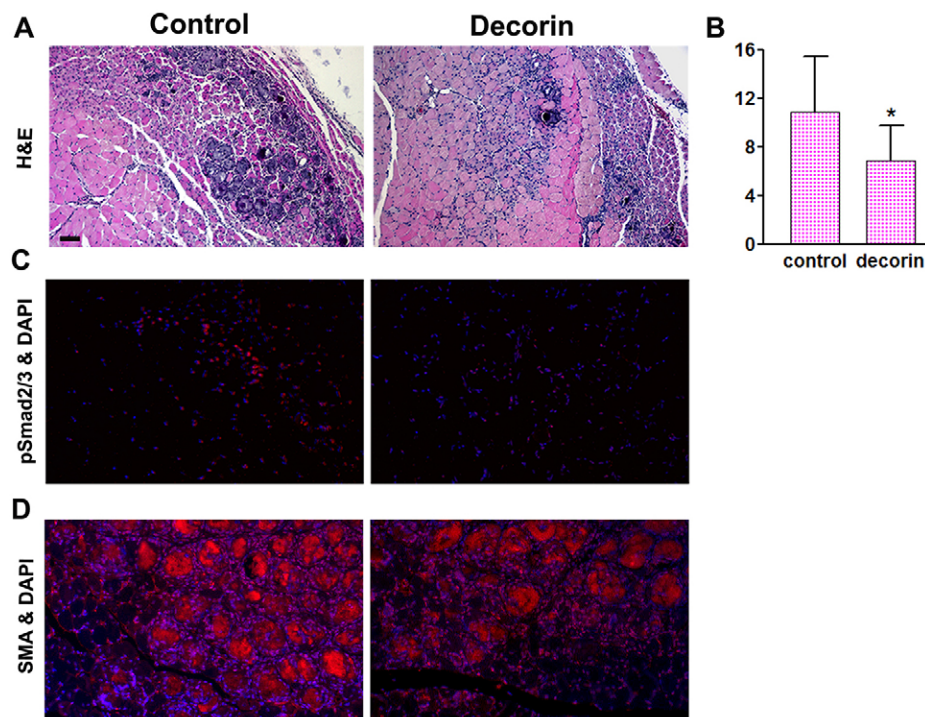
Fig. 5. Inhibition of pSmad signaling reduces muscle necrosis in Sharp-1$^{-/-}$ mutants. (A) Decorin, or the control vehicle (PBS) was injected into Sharp-1$^{-/-}$ muscles 7 days after injury and cross sections were analyzed at D10 by H&E staining. Decorin-injected muscles show a striking reduction of muscle pathology compared with the contralateral injured muscles ($n=4$) that were injected with PBS. (B) The percentage of pathology in the absence and presence of decorin was determined as a ratio of the necrotic area to the total injured area of the muscle. Results shown are representative from four sets of mice. Data are means $\pm$ s.d.; *$P<0.05$. (C,D) Control and decorin-injected sections were immunostained with anti-pSmad2/3 (C) and anti-SMA (D) antibodies which revealed reduced pSmad2/3 signaling in decorin-injected muscles ($n=3$). Scale bar: 100 µm.

reporter, which contains a TGF-β response element from the plasminogen activator inhibitor-1 (PAI-1) promoter and has been widely used to monitor TGF-β and Smad signaling (Wrana et al., 1992). Co-expression of full-length Sharp-1 resulted in repression of Smad3-induced reporter activity. By contrast, the Sharp-1-bHLH mutant, which failed to interact with Smad3, was significantly less effective in repression of Smad3-dependent transcriptional activity (Fig. 7A). Conversely, reporter activity was increased in cells transfected with Sharp-1 siRNA (siSharp-1) relative to control cells transfected with scrambled siRNA (siRNA) confirming that endogenous Sharp-1 regulates Smad3 activity (Fig. 7B). To examine the mechanisms underlying the inhibitory
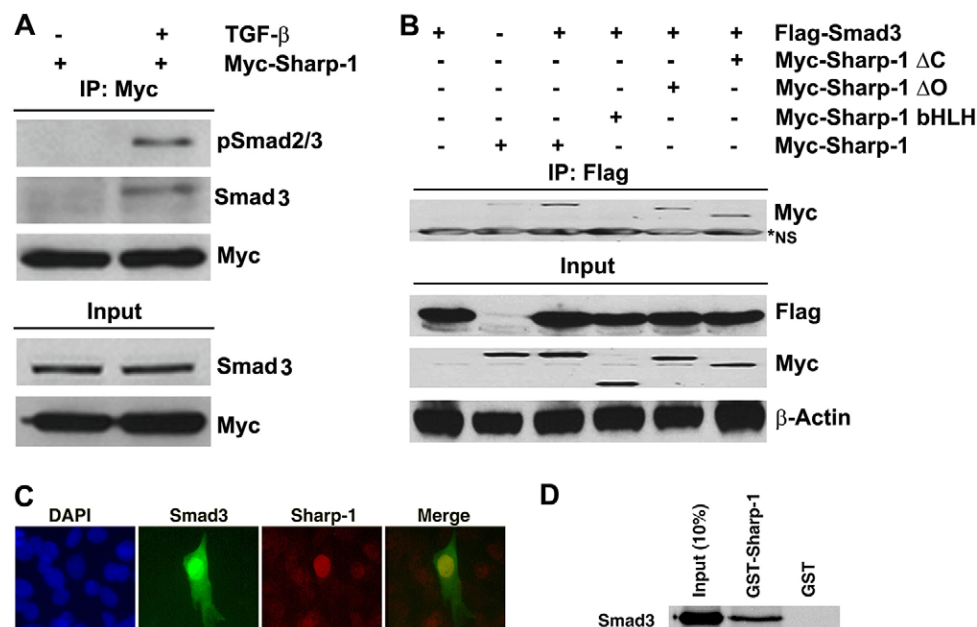

Fig. 6. Sharp-1 interacts with Smad3. (A) C2C12 cells were transfected with expression vectors for Myc–Sharp-1. Cells were left untreated or treated with TGF-β1 for 1 hour. Lysates were immunoprecipitated with anti-Myc agarose beads and immunoblotted with anti-pSmad2/3, Smad3 and Myc antibodies. Input shows expression of Smad3 and Sharp-1 in the lysates. (B) Cells were transfected with plasmids expressing FLAG–Smad3 and Myc–Sharp-1, Myc–Sharp-1 bHLH, Myc–Sharp-1 ΔO or Myc–Sharp-1 ΔC. 48 hours after transfection, lysates were immunoprecipitated with FLAG–agarose beads followed by western blot with anti-Myc antibody. Input shows expression of Smad3 and Sharp-1 in lysates. β-actin was used as an internal control. *NS, a non-specific IgG band. (C) C2C12 cells co-transfected with FLAG–Smad3 and Myc–Sharp-1 were analyzed using anti-FLAG and anti-Sharp-1 antibodies. Nuclei were stained with DAPI. (D) Equivalent amounts of GST–Sharp-1 or GST alone were incubated with ^{35}S-labeled *in vitro* translated Smad3. 10% of input was run on the gel as a control.
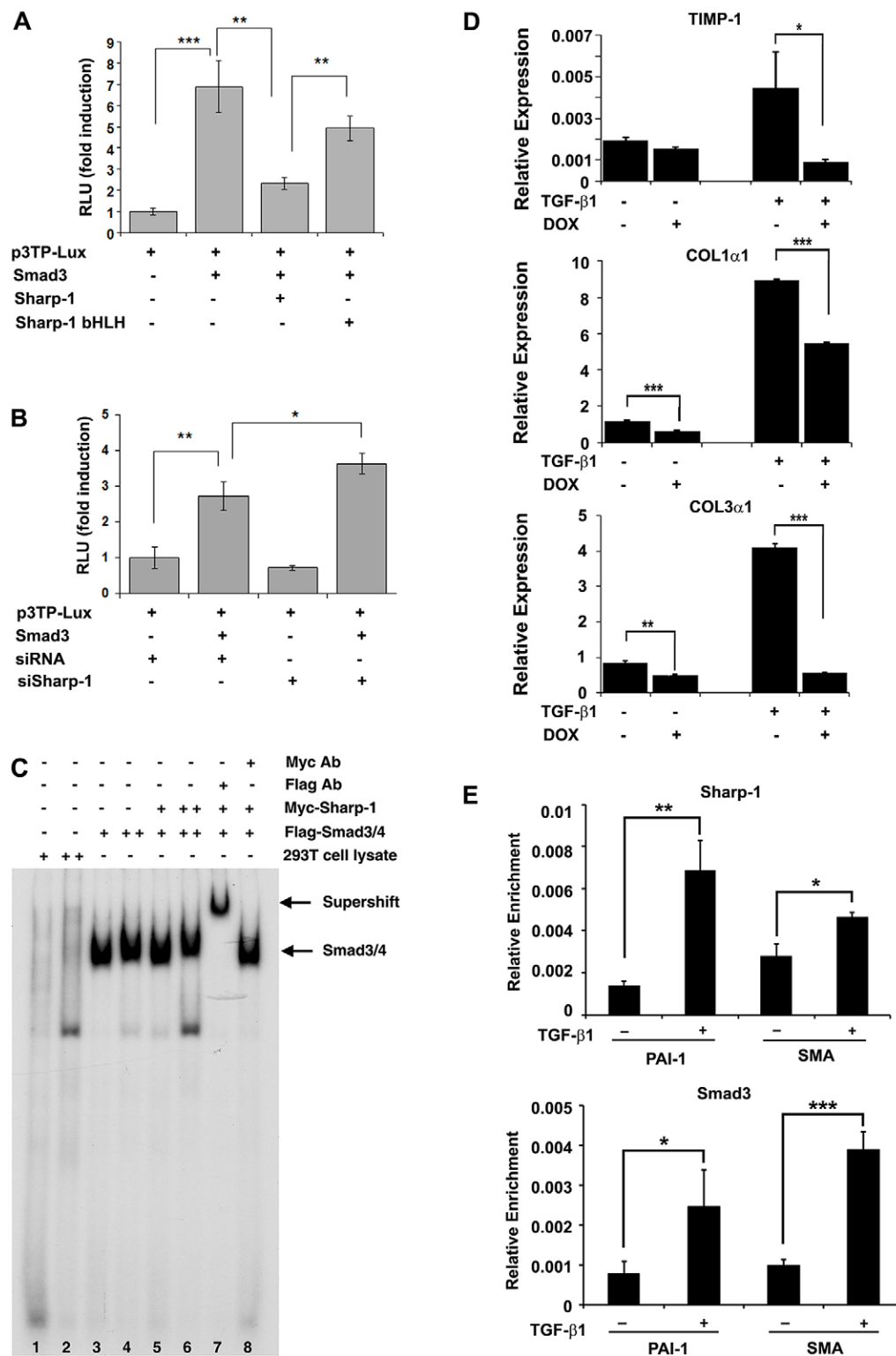
Fig. 7. Sharp-1 inhibits TGF-β signaling in myofibroblasts.
(A) Cells were transfected with reporter p3TP-Lux (200 ng) with Smad3 (100 ng) in the absence and presence of Sharp-1 (25 ng) and Sharp-1 bHLH (25 ng) as indicated. Cells were harvested 48 hr after transfection, and assayed for luciferase activity. Data are means ± s.d. (B) Cells were transfected with siSharp-1 and control scrambled siRNA at a final concentration of 100 nM. 24 hours later, Sharp-1 cells were transfected with p3TP-Lux (200 ng) and Smad3 (100 ng) as indicted in figure. Then, after a further 24 hours, luciferase activity was assayed. Data are means ± s.d. (C) ^{32}P-labeled SBE oligonucleotide was incubated with nuclear extracts prepared from non-transfected cells (lanes 1,2), increasing amount of FLAG–Smad3/4 (lanes 3, 4), and increasing amount of Smad3/4 and Myc–Sharp-1 (lanes 5,6). Supershift assays were carried out with anti-FLAG (lane 7) and anti-Myc-antibodies (lanes 7 and 8). (D) NIH3T3 cells were left uninduced or induced with doxycycline (DOX) and treated with TGF-β for 24 hours. The expression of COL1α1, COL3α1 and TIMP-1 was analyzed by Q-PCR. (E) ChIP assays were performed to determine occupancy of Sharp-1 and Smad2/3 at the PAI-1 and SMA promoters in the absence and presence of TGF-β. Data are means ± s.d.; *$P<0.05$; **$P<0.01$; ***$P<0.001$.

effect of Sharp-1 on Smad3 activity, we investigated whether Sharp-1 impacts the ability of Smad3 to bind to a Smad binding element (SBE). FLAG–Smad3 and FLAG–Smad4 were transfected in the absence or presence of Myc–Sharp-1. Nuclear extracts were incubated with a radioactive SBE probe. A complex containing Smad3 and Smad4 was evident on the SBE, which was supershifted with anti-FLAG, but not with anti-Myc antibody (Fig. 7C). Together, these data demonstrate that Sharp-1 does not

directly bind to the SBE, nor does it alter binding of Smad proteins to the SBE.

Myofibroblasts are heterogenous in origin and play a key role in tissue remodelling. They are characterized by synthesis of extracellular matrix (ECM) proteins and expression of SMA. Differentiation of fibroblasts and other cells to myofibroblasts requires TGF-β signaling which results in expression of ECM genes such as collagen1A1 (COL1α1), collagen1A2 (COL1α2),

and collagen3A1 (COL3α1) in a Smad3-dependent manner. In addition, TGF-β inhibits ECM degradation by increasing expression of matrix metalloprotease inhibitors such as tissue inhibitor of metalloprotease (TIMP-1). Given the increased TGF-β signaling and number of SMA$^+$ cells in Sharp-1 injured muscle, and the ability of Sharp-1 to antagonize Smad3 activity, we sought to determine whether Sharp-1 regulates TGF-β-induced ECM gene expression in myofibroblasts. NIH3T3 fibroblast cells that inducibly express Sharp-1 (Liu et al., 2010) were treated with TGF-β. As expected, the expression of collagen and TIMP-1 was induced by TGF-β (Fig. 7D). Interestingly, induction of Sharp-1 with doxycycline significantly inhibited TGF-β-mediated expression of COL1α1, COL3α1 and TIMP-1 (Fig. 7D). Similar results were seen when cells were treated with TGF-β for 48 hours (data not shown). The basal expression of COL1α1 and COL3α1 were suppressed by Sharp-1 even in the absence of exogenous TGF-β, indicating an impact of Sharp-1 on endogenous Smad3 activity. Moreover, chromatin immunoprecipitation assays showed that both Sharp-1 and Smad3 bind to the promoters of SMA and the plasminogen activator inhibitor PAI-1, which plays a significant role in fibrosis, in a TGF-β-responsive manner (Fig. 7E). Taken together, these results provide evidence that Sharp-1 antagonizes TGF-β signalling, probably by association with Smad3 and inhibition of its transcriptional activity in myofibroblast cells.

DISCUSSION

The results of this study demonstrate a novel role for Sharp-1 in tissue remodeling and muscle regeneration through its ability to limit TGF-β signaling in myofibroblasts. Although embryonic myogenesis does not appear to be overtly perturbed in Sharp-1$^{-/-}$ embryos, differentiation of myogenic precursor cells in response to injury is enhanced. Interestingly however, despite productive differentiation, Sharp-1$^{-/-}$ mice show a regeneration defect at late stages characterized by myonecrosis, proliferating myogenic and non-myogenic cells, calcification and fibrosis.

Postnatal myogenesis involves the interplay of many growth factors and cytokines, which act as positive or negative regulators of regeneration (Husmann et al., 1996; Chargé and Rudnicki, 2004). One such negative regulatory factor is TGF-β. TGF-β has been reported to inhibit myoblast proliferation and myogenic differentiation by inhibition of MyoD (Massagué et al., 1986; Allen and Boxhorn, 1987; Liu et al., 2001). Moreover, TGF-β also induces differentiation of fibroblasts into myofibroblasts in injured skeletal muscle (Li et al., 2004). The resulting overproliferation of myofibroblasts underlies deposition of extracellular matrix proteins, resulting in fibrosis and hindering complete regeneration of muscle tissue.

Expression and signaling of TGF-β are sustained at high levels in the mutants during regeneration. Intriguingly, however, myogenic differentiation is augmented at early stages in Sharp-1 mutant tissue, as seen by the increased number of eMHC$^+$ cells. This probably occurs because Sharp-1 is a potent inhibitor of MyoD activity and myogenic differentiation (Azmi et al., 2004; Morosetti et al., 2006; Ling et al., 2012; Wang et al., 2013). Its absence therefore would presumably result in increased MyoD activity that could counter the inhibitory effects of TGF-β at early stages in Sharp-1$^{-/-}$ mutants. Sustained TGF-β levels at a step subsequent to myogenic differentiation, probably results in more SMA$^+$ myofibroblasts and an increase in fibrosis in the mutant tissue. Previous studies have demonstrated that TGF-β-neutralizing antibodies and blockers can be used as potential antifibrotic agents (Isaka et al., 1996; Li et al., 2007). Blockade of

TGF-β with decorin indeed resulted in a nearly 35% decrease in myonecrosis in Sharp-1$^{-/-}$ mice. Therefore, enhanced TGF-β expression and signaling accounts, at least in part, for defective regeneration in Sharp-1$^{-/-}$ muscle.

Consistent with our findings, recent studies have shown an inverse correlation between Sharp-1 expression and TGF-β activity in breast and prostate cancer (Montagner et al., 2012; Sato et al., 2012). However, whether Sharp-1 directly inhibits TGF-β signaling, and the mechanisms underlying its inhibitory effect have not been reported. TGF-β signaling and Smad3 play a central role in fibrosis by enhancing expression of ECM genes such as collagens, decreasing expression of MMPs and increasing expression of MMP inhibitors (Flanders, 2004). Our data demonstrate that Sharp-1 directly interacts with Smad3, and inhibits its transcriptional activity. This antagonism is not due to direct competition for DNA binding because Sharp-1 does not bind to the Smad binding sites, nor does it impact binding of Smad proteins to DNA. It is plausible that Sharp-1 recruits co-factors such as HDAC1 (Garriga-Canut et al., 2001), Sirt1 (Fujimoto et al., 2007) or G9a (Ling et al., 2012; Wang et al., 2013) to block Smad3 transcriptional activity in a cell-type-specific manner.

Fibrosis poses a major obstacle to therapy, not only in muscle diseases, but in several other tissues as well. Although the role of TGF-β signalling in fibrosis is well established, much remains to be understood with regard to the mechanisms that lead to inappropriate TGF-β signaling and development of fibrosis. Our studies provide novel insights into the role of Sharp-1 in controlling TGF-β signaling in myofibroblasts and the development of anti-fibrotic therapies.

MATERIALS AND METHODS
Regeneration of skeletal muscle
Sharp-1$^{-/-}$ mice have been described previously (Rossner et al., 2008). Freeze-crush injury-induced regeneration was performed as described (Sun et al., 2007b). At least four mice were analyzed per time point (2, 5, 10 and 16 days after injury). All animal protocols followed institutional guidelines. For TGF-β blockade in vivo, quadriceps muscles were injured as described above. Seven days after injury, 20 μl (50 μg) of decorin (Sigma, St Louis, MO) was injected at six sites as described (Li et al., 2004). PBS (in 0.1% BSA) was injected as a control in the contralateral injured muscle. Muscles were collected 3 days after decorin injection and analyzed histologically.

Antibodies
Anti-MyoD and anti-pSmad2/3 antibodies used for immunohistochemistry were from Santa Cruz, Dallas, TX; anti-TGF-β was from Novocastra, Buffalo Grove, IL; anti β-actin from Sigma; anti-EF1α from Upstate Biotechnology Inc., Lake Placid, NY; anti-Pax7 and anti-eMHC from Developmental Studies Hybridoma Bank; anti-SMA from Sigma; anti phospho-Smad2/3 (Ser465/467) antibody from Millipore, Billerica, MA; anti-mouse and anti-rabbit Alexa Fluor secondary antibodies from Molecular Probes, Eugene, OR; anti-mouse and anti-rabbit HRP-conjugated secondary antibodies from Sigma.

Histology and immunohistochemistry
Serial cross-sections (8 μm thick) were collected along the entire length of embedded muscle tissues, and one out of every ten slides was stained with hematoxylin and eosin (HE) for identification of the largest damaged area. Sections from both genotypes with comparable damaged area were used for histology and immunohistochemistry. Immunohistochemistry was performed as described previously (Sun et al., 2007b) and visualized using the VECTASTAIN Elite ABC kit (Vector Laboratories, Burlingame, CA). Staining without primary antibody served as a negative control. For immunofluorescence, paraffin-embedded sections were incubated with

appropriate primary antibody followed by detection with secondary antibody from Alexa Fluor and analyzed under a fluorescence microscope. Masson's Trichrome staining was performed using a kit (Diagnostics Biosystem, Pleasanton, CA). For Alizarin Red staining, sections were deparaffinized and stained for 30 seconds in 2% Alizarin Red solution followed by washes in acetone, acetone:xylene (1:1), xylene and were then mounted. Calcium deposits were viewed as orange-red staining.

Morphological analysis
Damaged areas and cross section areas (CSAs, μm^2) were measured using ImageJ software (version 1.36b, NIH). For measuring the CSA, quadriceps from four mice (3 months old) of each genotype were analyzed and at least 500 myofibers per muscle were measured. The extent of pathology with or without decorin treatment was determined as a ratio of the necrotic area of the injured muscle to the total area of the injured muscle section.

Regeneration index
Regeneration was assessed by counting the number of eMHC[+] fibers normalized to the total number of nuclei in five to ten randomly selected fields as described previously (Sun et al., 2007b).

Satellite cell number
Paraffin sections of quadriceps muscle from 2-month-old mice were stained with anti-Pax7 antibody and counterstained with hematoxylin. Both myonuclei and Pax7^{+} nuclei were counted from several random fields for each animal, and the percentage of satellite cells was calculated. At least 500 nuclei were counted for each animal, and the data presented are an average of four animals.

Immunofluorescence analysis
Paraffin embedded sections were deparaffinised in Histoclear (SUPPLIER?). After antigen retrieval, sections were incubated in blocking buffer for 1 hour, followed by staining with primary antibodies against SMA and MyoD and detection with Alexa Fluor dye-conjugated secondary antibodies. Sections were mounted in mounting medium containing DAPI (Vectashield H-1200, Vector Laboratories, Burlingame, CA) and imaged using a Zeiss AX10 microscope. To determine the localization of Sharp-1 and Smad3, C2C12 cells were seeded in chamber slides at ∼30% confluence. Cells were transfected with Myc–Sharp-1, FLAG–Smad3 alone or together. 24 hours after transfection, cells were fixed in 4% paraformaldehyde, treated with 0.5% Triton X-100 and washed with PBS. After blocking (10% BSA in PBS), slides were incubated with Myc and FLAG antibodies followed by fluorescence-conjugated secondary antibodies. Cells were mounted in DAPI containing mounting medium from Vectastain (Vector Laboratories) and viewed under a fluorescence microscope.

Plasmids, cell culture, luciferase assays and Sharp-1 knockdown
FLAG–Smad2, FLAG–Smad3 and FLAG–Smad4 were kindly provided by Rik Derynck (University of California San Francisco, San Francisco, CA); 3TP-Lux was kindly provided by Jeff Wrana (Lunenfeld-Tanenbaum Research Institute, Mount Sinai Hospital, Toronto, Canada); Myc–Sharp-1 and GST–Sharp-1 have been described previously (Ling et al., 2012). C2C12 and 293T cells were maintained in Dulbecco's modified Eagle's medium (DMEM) containing 20% and 10% fetal bovine serum (FBS), respectively. For differentiation, C2C12 cells were cultured in DMEM with 2% horse serum. NIH3T3 cells were maintained in DMEM containing 10% bovine serum (BS). Sharp-1-inducible NIH3T3 cells have been described and were treated with 2 $\mu g/ml$ doxycycline (DOX) for 24 and 48 hours to induce Sharp-1 (Liu et al., 2010). Transient transfections were performed using Lipofectamine Plus or Lipofectamine 2000 (Invitrogen, Grand Island, NY). For reporter assays, cells were transfected with the reporter 3TP-Lux and various plasmid constructs as indicated in the figures along with 5 ng of Renilla luciferase as an internal control. Empty expression vector was added to normalize the amount of total DNA. 48 hours after transfection, luciferase assays were performed using the dual luciferase system (Promega, Fitchburg, WI). All transfections were performed in triplicate and repeated at least twice. Values are reported as means ± s.d. To knock down Sharp-1, C2C12 cells were transfected with

100 nM siRNA specific for mouse Sharp-1 (Qiagen, Valencia, CA), or with control scrambled siRNA using Lipofectamine RNAiMAX (Invitrogen, Grand Island, NY). 24 hours after transfection, siRNA knockdown cells were transfected with the reporter and plasmid constructs and luciferase activity was measured as described above. For all experiments, TGF-β was used at 5 ng/ml.

Co-immunoprecipitation and GST-pull down assays
Co-immunoprecipitation and GST-pull down assays were done as described (Sun and Taneja, 2000). Briefly, for Co-IP assays, cells were transfected with Myc–Sharp-1. Then, 24 hours later, cells were treated for 1 hour with 5 ng/ml TGF-β before lysing. Control cells were not treated with TGF-β. Sharp-1 was immunoprecipitated using Myc–agarose beads (Sigma) and probed for endogenous pSmad2/3 and Smad3. To map the interaction domains between Sharp-1 and Smad3, cells were transfected with full-length Myc–Sharp-1 and deletion mutants Sharp-1 bHLH, Sharp-1 ΔO or Sharp-1 ΔC (Ling et al., 2012) together with FLAG-Smad3. 48 hours later, cells were washed twice with cold PBS, lysed in 50 mM Tris-HCl, pH 8.0, 50 mM NaCl, 1 mM EDTA, 0.1% Triton X-100, 0.5 mM PMSF and protease inhibitors (Roche Applied Science, Mannheim, Germany). Equal amounts of total protein were loaded for western blotting. Lysates were incubated with FLAG-agarose beads (Sigma) and analyzed by western blotting using anti-Myc antibody (1:1000, Sigma). For GST-pull down assays, Smad3 was translated in vitro and labeled with [^{35}S]methionine using the TNT-coupled reticulocyte lysate system (Promega, Fitchburg, WI). ^{35}S-labeled Smad3 was incubated with purified GST-Sharp-1 or GST in binding buffer. Samples were run on SDS gels and detected by autoradiography (Sun and Taneja, 2000).

Electrophoretic mobility shift assay (EMSA)
FLAG–Smad3, FLAG–Smad4 and Myc–Sharp-1 were transfected and 48 hours later, cells were stimulated with TGF-β (5 ng/ml) for 1 hour. Nuclear extracts prepared from transfected samples were incubated with ^{32}P-labeled SBE probe (5′-CTCTATCAATTGGTCTAGACTTAACC-GGA). Binding reactions contained 40,000 cpm probe, 1 μg of poly(dI-dC), 10 mM HEPES, pH 7.9, 80 mM KCl, 0.1 mM EDTA, 5 mM MgCl$_2$, 0.5 mM dithiothreitol, 10% glycerol and increasing amounts of nuclear extract (+ 1.5 μg; ++ 3 μg). The reaction was incubated in room temperature for 20 minutes and fractionated on 5% polyacrylamide gels. For supershift, antibodies were added and incubated for 10 minutes following incubation with radiolabeled probe.

Chromatin immunoprecipitation assay
C2C12 cells at 80% confluency were cultured in differentiation medium for 2 days in the absence or presence of 5 ng/ml TGF-β. Cells were fixed with 1% formaldehyde and ChIP assays were performed using Millipore ChIP kit (Billerica, Massachusetts). 2 μg of anti-Sharp-1 and anti-Smad3 antibodies (Santa Cruz) were used. DNA was amplified by quantitative RT-PCR (Roche Applied Science, Mannheim, Germany) with primers specific to mouse PAI-1 promoter (−600 to −800 bp) containing TGFβ/SMAD-responsive regions. Primer sequences for mouse PAI-1 are: 5′ CACAAAGAGCGAGCCCTCAG-3′ and 5′-CCAGAGGGCATGAAA-TGTGC-3′. Primers for SMA promoter have been described previously (Elberg et al., 2008).

Quantitative real-time PCR
Q-PCR was done as described (Ling et al., 2012). Briefly, RNA was reverse transcribed using iSCRIPT (Bio-Rad, Hercules, CA) and Q-PCR was performed using Roche Sybr green in LC480 (Roche Applied Science, Mannheim, Germany). Mouse Sharp-1 was amplified using the following primers: Forward 5′-AACACTGGGGCATTTGGAGA-3′ and Reverse 5′-TGGACCGGCGATTTCAGAG-3′. Primers for TIMP-1, COL1α1 and COL3α1 have been described previously (Meng et al., 2010; and Uezumi et al., 2011).

Statistical analysis
Student's t-test was used to perform statistical analysis and $P<0.05$ was considered significant (*$P<0.05$; **$P<0.01$; ***$P<0.001$).

References

Allen, R. E. and Boxhorn, L. K. (1987). Inhibition of skeletal muscle satellite cell differentiation by transforming growth factor-beta. *J. Cell. Physiol.* **133**, 567-572.

Azmi, S., Sun, H., Ozog, A. and Taneja, R. (2003). mSharp-1/DEC2, a basic helix-loop-helix protein functions as a transcriptional repressor of E box activity and Stra13 expression. *J. Biol. Chem.* **278**, 20098-20109.

Azmi, S., Ozog, A. and Taneja, R. (2004). Sharp-1/DEC2 inhibits skeletal muscle differentiation through repression of myogenic transcription factors. *J. Biol. Chem.* **279**, 52643-52652.

Barnard, J. A., Lyons, R. M. and Moses, H. L. (1990). The cell biology of transforming growth factor beta. *Biochim. Biophys. Acta* **1032**, 79-87.

Bernasconi, P., Torchiana, E., Confalonieri, P., Brugnoni, R., Barresi, R., Mora, M., Cornelio, F., Morandi, L. and Mantegazza, R. (1995). Expression of transforming growth factor-beta 1 in dystrophic patient muscles correlates with fibrosis. Pathogenetic role of a fibrogenic cytokine. *J. Clin. Invest.* **96**, 1137-1144.

Bernasconi, P., Di Blasi, C., Mora, M., Morandi, L., Galbiati, S., Confalonieri, P., Cornelio, F. and Mantegazza, R. (1999). Transforming growth factor-beta1 and fibrosis in congenital muscular dystrophies. *Neuromuscul. Disord.* **9**, 28-33.

Border, W. A. and Noble, N. A. (1994). Transforming growth factor β in tissue fibrosis. *N. Engl. J. Med.* **331**, 1286-1292.

Border, W. A. and Ruoslahti, E. (1992). Transforming growth factor-β in disease: the dark side of tissue repair. *J. Clin. Invest.* **90**, 1-7.

Chargé, S. B. and Rudnicki, M. A. (2004). Cellular and molecular regulation of muscle regeneration. *Physiol. Rev.* **84**, 209-238.

Cohn, R. D., van Erp, C., Habashi, J. P., Soleimani, A. A., Klein, E. C., Lisi, M. T., Gamradt, M., ap Rhys, C. M., Holm, T. M., Loeys, B. L. et al. (2007). Angiotensin II type 1 receptor blockade attenuates TGF-beta-induced failure of muscle regeneration in multiple myopathic states. *Nat. Med.* **13**, 204-210.

Desmoulière, A., Geinoz, A., Gabbiani, F. and Gabbiani, G. (1993). Transforming growth factor-beta 1 induces alpha-smooth muscle actin expression in granulation tissue myofibroblasts and in quiescent and growing cultured fibroblasts. *J. Cell Biol.* **122**, 103-111.

Elberg, G., Chen, L., Elberg, D., Chan, M. D., Logan, C. J. and Turman, M. A. (2008). MKL1 mediates TGF-beta1-induced alpha-smooth muscle actin expression in human renal epithelial cells. *Am. J. Physiol. Renal Physiol.* **294**, F1116-F1128.

Flanders, K. C. (2004). Smad3 as a mediator of the fibrotic response. *Int. J. Exp. Pathol.* **85**, 47-64.

Fujimoto, K., Hamaguchi, H., Hashiba, T., Nakamura, T., Kawamoto, T., Sato, F., Noshiro, M., Bhawal, U. K., Suardita, K. and Kato, Y. (2007). Transcriptional repression by the basic helix-loop-helix protein Dec2: multiple mechanisms through E-box elements. *Int. J. Mol. Med.* **19**, 925-932.

Garriga-Canut, M., Roopra, A. and Buckley, N. J. (2001). The basic helix-loop-helix protein, sharp-1, represses transcription by a histone deacetylase-dependent and histone deacetylase-independent mechanism. *J. Biol. Chem.* **276**, 14821-14828.

Grinnell, F. (1994). Fibroblasts, myofibroblasts, and wound contraction. *J. Cell Biol.* **124**, 401-404.

Gulbagci, N. T., Li, L., Ling, B., Gopinadhan, S., Walsh, M., Rossner, M., Nave, K. A. and Taneja, R. (2009). SHARP1/DEC2 inhibits adipogenic differentiation by regulating the activity of C/EBP. *EMBO Rep.* **10**, 79-86.

Hawke, T. J. and Garry, D. J. (2001). Myogenic satellite cells: physiology to molecular biology. *J. Appl. Physiol.* **91**, 534-551.

Heldin, C. H., Miyazono, K. and ten Dijke, P. (1997). TGF-β signalling from cell membrane to nucleus through SMAD proteins. *Nature* **390**, 465-471.

Huard, J., Li, Y. and Fu, F. H. (2002). Muscle injuries and repair: current trends in research. *J. Bone Joint Surg. Am.* **84-A**, 822-832.

Husmann, I., Soulet, L., Gautron, J., Martelly, I. and Barritault, D. (1996). Growth factors in skeletal muscle regeneration. *Cytokine Growth Factor Rev.* **7**, 249-258.

Isaka, Y., Brees, D. K., Ikegaya, K., Kaneda, Y., Imai, E., Noble, N. A. and Border, W. A. (1996). Gene therapy by skeletal muscle expression of decorin prevents fibrotic disease in rat kidney. *Nat. Med.* **2**, 418-423.

Lefaucheur, J. P. and Sébille, A. (1995). Muscle regeneration following injury can be modified in vivo by immune neutralization of basic fibroblast growth factor, transforming growth factor beta 1 or insulin-like growth factor I. *J. Neuroimmunol.* **57**, 85-91.

Li, Y., Foster, W., Deasy, B. M., Chan, Y., Prisk, V., Tang, Y., Cummins, J. and Huard, J. (2004). Transforming growth factor-beta1 induces the differentiation of myogenic cells into fibrotic cells in injured skeletal muscle: a key event in muscle fibrogenesis. *Am. J. Pathol.* **164**, 1007-1019.

Li, Y., Li, J., Zhu, J., Sun, B., Branca, M., Tang, Y., Foster, W., Xiao, X. and Huard, J. (2007). Decorin gene transfer promotes muscle cell differentiation and muscle regeneration. *Mol. Ther.* **15**, 1616-1622.

Ling, B. M., Gopinadhan, S., Kok, W. K., Shankar, S. R., Gopal, P., Bharathy, N., Wang, Y. and Taneja, R. (2012). G9a mediates Sharp-1-dependent inhibition of skeletal muscle differentiation. *Mol. Biol. Cell* **23**, 4778-4785.

Liu, D., Black, B. L. and Derynck, R. (2001). TGF-beta inhibits muscle differentiation through functional repression of myogenic transcription factors by Smad3. *Genes Dev.* **15**, 2950-2966.

Liu, J. J., Chung, T. K., Li, J. and Taneja, R. (2010). Sharp-1 modulates the cellular response to DNA damage. *FEBS Lett.* **584**, 619-624.

Massagué, J., Cheifetz, S., Endo, T. and Nadal-Ginard, B. (1986). Type beta transforming growth factor is an inhibitor of myogenic differentiation. *Proc. Natl. Acad. Sci. USA* **83**, 8206-8210.

Massaous, J. and Hata, A. (1997). TGF-β signalling through the Smad pathway. *Trends Cell Biol.* **7**, 187-192.

Meng, X. M., Huang, X. R., Chung, A. C., Qin, W., Shao, X., Igarashi, P., Ju, W., Bottinger, E. P. and Lan, H. Y. (2010). Smad2 protects against TGF-beta/Smad3-mediated renal fibrosis. *J. Am. Soc. Nephrol.* **21**, 1477-1487.

Montagner, M., Enzo, E., Forcato, M., Zanconato, F., Parenti, A., Rampazzo, E., Basso, G., Leo, G., Rosato, A., Bicciato, S. et al. (2012). SHARP1 suppresses breast cancer metastasis by promoting degradation of hypoxia-inducible factors. *Nature* **487**, 380-384.

Morosetti, R., Mirabella, M., Gliubizzi, C., Broccolini, A., De Angelis, L., Tagliafico, E., Sampaolesi, M., Gidaro, T., Papacci, M., Roncaglia, E. et al. (2006). MyoD expression restores defective myogenic differentiation of human mesoangioblasts from inclusion-body myositis muscle. *Proc. Natl. Acad. Sci. USA* **103**, 16995-17000.

Moses, H. L., Yang, E. Y. and Pietenpol, J. A. (1990). TGF-beta stimulation and inhibition of cell proliferation: new mechanistic insights. *Cell* **63**, 245-247.

Murakami, N., McLennan, I. S., Nonaka, I., Koishi, K., Baker, C. and Hammond-Tooke, G. (1999). Transforming growth factor-beta2 is elevated in skeletal muscle disorders. *Muscle Nerve* **22**, 889-898.

Rossner, M. J., Oster, H., Wichert, S. P., Reinecke, L., Wehr, M. C., Reinecke, J., Eichele, G., Taneja, R. and Nave, K. A. (2008). Disturbed clockwork resetting in Sharp-1 and Sharp-2 single and double mutant mice. *PLoS ONE* **3**, e2762.

Sato, F., Kawamura, H., Wu, Y., Sato, H., Jin, D., Bhawal, U. K., Kawamoto, T., Fujimoto, K., Noshiro, M., Seino, H. et al. (2012). The basic helix-loop-helix transcription factor DEC2 inhibits TGF-β-induced tumor progression in human pancreatic cancer BxPC-3 cells. *Int. J. Mol. Med.* **30**, 495-501.

Serini, G. and Gabbiani, G. (1996). Modulation of α-smooth muscle actin expression in fibroblasts by transforming growth factor-β isoforms: an in vivo and in vitro study. *Wound Repair Regen.* **4**, 278-287.

Serini, G., Bochaton-Piallat, M. L., Ropraz, P., Geinoz, A., Borsi, L., Zardi, L. and Gabbiani, G. (1998). The fibronectin domain ED-A is crucial for myofibroblastic phenotype induction by transforming growth factor-beta1. *J. Cell Biol.* **142**, 873-881.

Sun, H. and Taneja, R. (2000). Stra13 expression is associated with growth arrest and represses transcription through histone deacetylase (HDAC)-dependent and HDAC-independent mechanisms. *Proc. Natl. Acad. Sci. USA* **97**, 4058-4063.

Sun, H., Ghaffari, S. and Taneja, R. (2007a). bHLH-Orange transcription factors in development and cancer. *Translational Oncogenomics* **2**, 107-120.

Sun, H., Li, L., Vercherat, C., Gulbagci, N. T., Acharjee, S., Li, J., Chung, T. K., Thin, T. H. and Taneja, R. (2007b). Stra13 regulates satellite cell activation by antagonizing Notch signaling. *J. Cell Biol.* **177**, 647-657.

Uezumi, A., Ito, T., Morikawa, D., Shimizu, N., Yoneda, T., Segawa, M., Yamaguchi, M., Ogawa, R., Matev, M. M., Miyagoe-Suzuki, Y. et al. (2011). Fibrosis and adipogenesis originate from a common mesenchymal progenitor in skeletal muscle. *J. Cell Sci.* **124**, 3654-3664.

Wang, Y., Shankar, S. R., Kher, D., Ling, B. M. and Taneja, R. (2013). Sumoylation of the basic helix-loop-helix transcription factor sharp-1 regulates recruitment of the histone methyltransferase G9a and function in myogenesis. *J. Biol. Chem.* **288**, 17654-17662.

Wrana, J. L., Attisano, L., Cárcamo, J., Zentella, A., Doody, J., Laiho, M., Wang, X. F. and Massagué, J. (1992). TGF beta signals through a heteromeric protein kinase receptor complex. *Cell* **71**, 1003-1014.

Yamada, K. and Miyamoto, K. (2005). Basic helix-loop-helix transcription factors, BHLHB2 and BHLHB3; their gene expressions are regulated by multiple extracellular stimuli. *Front. Biosci.* **10**, 3151-3171.

Zhu, J., Li, Y., Shen, W., Qiao, C., Ambrosio, F., Lavasani, M., Nozaki, M., Branca, M. F. and Huard, J. (2007). Relationships between transforming growth factor-beta1, myostatin, and decorin: implications for skeletal muscle fibrosis. *J. Biol. Chem.* **282**, 25852-25863.